NIH Public Access
Author Manuscript
Nat Med. Author manuscript; available in PMC 2014 June 10.

Published in final edited form as:
Nat Med. 2013 September ; 19(9): 1132–1140. doi:10.1038/nm.3265.

Activation of the Nlrp3 inflammasome in infiltrating macrophages by endocannabinoids mediates beta cell loss in type 2 diabetes

Tony Jourdan[1], **Grzegorz Godlewski**[1], **Resat Cinar**[1], **Adeline Bertola**[2], **Gergö Szanda**[1], **Jie Liu**[1], **Joseph Tarn**[1], **Tiffany Han**[1], **Bani Mukhopadhyay**[1], **Monica C Skarulis**[1], **Cynthia Ju**[4], **Myriam Aouadis**[5], **Michael P Czech**[5], and **George Kunos**[1]

[1] Laboratory of Physiologic Studies, National Institute on Alcohol Abuse and Alcoholism, US National Institutes or Health, Bcthcsda, Maryland [2]Laboratory of Liver Diseases, National Institute on Alcohol Abuse and Alcoholism, US National Institutes of Health, Belhesda, Maryland [3]Diabetes, Endocrinology and Obesity Branch. National Institute of Diabetes and Digestive and Kidney Diseases, US National Institutes ol Health. Bcthcsda, Maryland [4]Skaggs School of Pharmacy and Pharmaceutical Sciences, University of Colorado Anschutz Medical Campus, Aurora, Colorado [5]Program in Molecular Medicine, University of Massachusetts Medical School, Worcester, Massachusetts

Abstract

Type 2 diabetes mellitus (T2DM) progresses from compensated insulin resistance to beta ceil failure resulting in uncompensated hyperglycemia, a process replicated in the Zucker diabetic fatty (ZDF) rat. The Nlrp3 inflammasome has been implicated in obesity-induced insulin resistance and beta cell failure. Endocannabinoids contribute to insuiin resistance through activation of peripheral CB_1 receptors (CB_1Rs) and also promote beta cell failure. Here we show that beta cell failure in adult ZDF rats is not associated with CB_1R signaling in beta ceils, but rather in M1 macrophages infiltrating into pancreatic islets, and that this leads to activation of the Nlrp3-ASC inflammasome in the macrophages. These effects are replicated *in vitro* by incubating wild-type human or rodent macrophages, but not macrophages from CB_1R-deficient [*Cnr1*$^{-/-}$) or *Nlrp3*$^{-/-}$ mice, with the endocannabinoid anandamide. Peripheral CB_1R blockade, *in vivo* depletion of macrophages or macrophage-specific knockdown of CB_1R reverses or prevents these changes and restores normoglycemia and glucose-induced insulin secretion. These findings implicate endocannabinoids

© 2013 Nature America, Inc. All rights reserved.

Correspondence should be addressed to T.J. (jourdant@mail.nih.gov) or G.K. (george.kunos@nih.gov)..

AUTHOR CONTRIBUTIONS

T.J. and G.K. designed and carried out experiments, analyzed results and wrote the manuscript. G.G. performed the surgery and the clamp experiments, R,G. conducted liquid chromatography–tandem mass spectrometry endocannahinoid measurements, A.B. did some of the imrnunohistochemistry and FACS analyses, G.S. did western blotting and PGR assays, J.L. J.T and B.M. assisted with cell culture experiments, T.H. did the work on macrophage depletion, MG.S. provided human blood samples, C.J. provided clodrunate liposomes, T.J. and M.A. designed and tested the GeRPs, and M.A. and M.P G. provided GeRPs, All authors had access to the manuscript and agreed wilh the final version.

Any Supplementary Information and Source Data files are available in the online version of the paper.

COMPETING FINANCIAL INTERESTS

The authors declare no competing financial interests.

NIH-PA Author Manuscript
NIH-PA Author Manuscript
NIH-PA Author Manuscript

NIH-PA Author Manuscript

NIH-PA Author Manuscript

NIH-PA Author Manuscript

and inflammasome activation in beta cell failure and identify macrophage-expressed CB_1R as a therapeutic target in T2DM.

T2DM typically progresses from a slate of prediabetes (that is, insulin resistance coupled with hyperinsulincmia that is able lo maintain euglycemia) to an overt stale of diabetes thai is caused by beta cell failure and impaired insulin secretion and thus marked by fasting hyperglycemia[1]. The pathogenic role of inflammation in both stages of T2DM is increasingly recognized. Adipose tissue inflammation contributes to insulin resistance through proinflammatory cytokines such as lumor necrosis factor-α (TNF-α) and inlerleukin-6 (1L-6) (ref. 2), and infiltration of proinflammatory cells into pancreatic islets of subjects and animals with diabetes may contribute lo beta cell failure[3]. Furthermore, the Nlrp3 inflammasome, a protein complex involved in the proteolytic activation ofcaspase-1 and inlerleukin-lβ (IL-β) secretion, has been implicated in the pathogenesis of diabetogenic insulitis[4–7].

Endocannabinoids, or lipid ligands of G protein–coupled CB_1R and CB_2R, produce a broad range of biological effects[8], CB_1R activation promotes food intake[9], increases lipogenesis in adipose tissue[10] and liver[11,12] and induces insulin resistance and dyslipidemia[13,14]. These effects suggest that an overactive endocannabinoid-CB_1R system contributes to the development of visceral obesity and its complications[15]. Accordingly, chronic CB_1R blockade reduces body weight and improves obesity-related insulin resistance, dyslipidemia and fatty liver both in obese rodents[16,17] and in humans[18,19]. CB_1R blockade also improves giycemic control as a monotherapy in drug-naive subjects with T2DM[20]. However, the therapeutic development of CB_1R antagonists or inverse agonists has been halted due to adverse psychiatric effects, which are likely caused by central activation of these receptors as opposed to their peripheral effects[21].

In mice with high-fat diet-induced obesity (DIO), selective blockade of peripheral CB_1R replicates the metabolic benefit of global GB_1R blockade without adverse behavioral effects[22,23]. DIO mice are insulin resistant, but their fasting blood glucose is only moderately higher compared lo wild-type mice owing to compensatory hyperinsuline-mia. Leptin-resistant Zucker fatty (*fa/fa*) rats are also obese (due to a recessive mutation in the gene encoding the leptin receptor) and are similarly insulin resistant but remain normoglycemic as a result of compensatory beta cell growth[24]. In contrast, the ZDF rat, derived from the Zucker fatty rat by inbreeding for fasting hyperglycemia, replicates the natural history ofhuman T2DM[25]. Young ZDF rats (up to 7 weeks old) are insulin resistant with hyperinsulinemia and normoglycemia but become extremely hyperglycemic with decreasing hyperinsulinemia by 9 weeks of age, which reflects rapidly progressing beta cell failure. Treatment of ZD1; rats with brain-penetrant CB_1R antagonists was recently reported to reduce their hyperglycemia and increase both plasma and islet insulin levels, suggesting beta cell protection, although the underlying mechanisms, including the tissue localization of the CB_1Rs involved and their downstream targets, remain unclear[26]. One possible target is CB_1Rs on beta cells, the activation of which can facilitate proapoptotie signaling through an autocrine mechanism[27] similar to an inflammasome-mediated autocrine signaling implicated in lipotoxic beta cell death[28,29]. Alternatively, activation of macrophage CB_1Rs can induce

NIH-PA Author Manuscript

NIH-PA Author Manuscript

NIH-PA Author Manuscript

transmigration and proinflammatory signaling[30], which could kill beta cells through a paracrine mechanism, finally, as central mechanisms may regulate beta cell function[31] and survival[32], and endocannabinoids can also influence glycemic control through activation of CB_1Rs in the CNS[33], they may induce beta cell death through neural input from the brain.

Here we demonstrate, using a combination of pharmacological and genetic tools, that beta cell loss in ZDF rats is induced through a paracrine mechanism by inflammatory cytokines, including IL-1β released from infiltrating M1 macrophages as a result of CB_1R-mediated selective activation of the Nlrp3-ASC inflammasome in the macrophages. These effects can be prevented by peripheral CB_1R blockade or selective knockdown of macrophage CB_1R.

RESULTS

Peripheral CB_1R blockade delays the progression of T2DM

We treated 8-week-old male diabetic ZDF rats orally with the non–brain-penetrant CB_1R inverse agonist JDS037 (ref. 23) or vehicle for 28 d. Relative to lean littermates, vehicle-treated ZDF rats were obese and hyperphagic (**Fig. 1a**), had higher hepatic concentration of triglycerides and higher expression of theiipogenic genes *Fas* and *Scdl* (**Fig. 1b**) and had overt diabetes, indicated by pronounced hyperglycemia, higher hemoglobin A1c (HbA1c) levels and moderate hyperinsulinemia (**Fig, 1c**). Furthermore, they had extremely high plasma triglyceride and cholesterol concentrations (**Supplementary Table 1**).

Chronic ID5037 treatment of ZDF rats did not affect body weight or adiposity and was associated with a slightly lower amount of food intake than in vehicle-treated ZDF rats (**Fig. 1a**), whe reas the steatosis, the associated hepatocellular damage and the lipogenic gene expression were significantly lower (**Fig. 1b**). JD5037-treated ZDF rats were euglycemic, whereas their plasma insulin and C-peptide levels were paradoxically higher compared to vehicle-treated ZDF rats (**Fig. 1c**), suggesting improved beta cell function and survival. The inactive diastereomer of JD5037 (ref. 23) did not affect plasma glucose, insulin or C-peptide levels (**Supplementary Fig. 1**). Normoglycemia coupled with hyperinsulinemia in JD5037-treated rats suggests continued insulin resistance. Indeed, the insulin resistance of ZDF rats, which was primarily due to decreased peripheral glucose uptake, was not significantly affected by JD5037, as revealed by euglycemic-hyperinsulinemicclamps (**Fig. 1d**).

JD5037 treatment also normalized insulin mRNA and protein levels in ZDF islets, probably by preventing beta cell apoptosis. This is indicated by the lower number of TUNEL-positive islet cells (**Fig. 2a**), the lower expression of the apoplotic markers *Bakl*, *Bax*, *Fas*, *Faslg* and *Tnfrsfla* and the higher expression of the antiapoptotic markers *Bcl2* and *Bc2l1* as compared to vehicle-treated ZDF rats (**Supplementary Fig. 2a**). At the same time, JD5037 treatment was associated with greater beta cell mass compared to that in vehicle-treated rats (**Supplementary Fig. 2b**), probably as a result of higher gene expression of transcription factors involved in beta cell survival, such as *Pdx1*, *Mafa* and *Neurog3* (**Supplementary Fig 2c**), and also reflected by more insulin-producing beta cells expressing the proliferation marker Ki67 (**Supplementary Fig. 2d**). The higher expression of *Cnr1* and amounts of anandamide in islets of ZDF compared to lean littermates was not observed in JD5037-treated ZDF rats (**Fig. 2a**).

NIH-PA Author Manuscript

NIH-PA Author Manuscript

NIH-PA Author Manuscript

The loss of insulin-producing beta cells in ZDF rats was paralleled by the absence of glucose-stimulated insulin secretion (CSIS), as assessed *in vivo* by measuring plasma insulin and C-peptide within 5 min of a glucose load and *in vitro* in isolated perfused islets. The basal hyperinsulinemia of JD5037-treated rats was similar to that in vehicle-treated ZDF rats, but it correlated with a normal GS1S response both *in vivo* and *in vitro* (**Fig. 2b**). In parallel, JD5037 treatment was associated with normal expression in pancreatic islets, of glucokinase (*Gck*) and of *Glut2* (*Slc2a2*) (**Fig, 2c**), which mediates glucose uptake by beta cells.

After we treated 6-week-old prediabetic ZDF rats with FD5037 daily for 3 months, their hyperglycemia was lower and its development much slower than in vehicle-treated age-matched ZDF rats, and the rapid decline in plasma insulin and C-peptide was largely prevented (**Fig. 2d**). Thus, peripheral CB_1R blockade delays the progression of T2DM and the loss ofbeta cell function.

CB_1R blockade reverses macrophage infiltration in ZDF islets

ZDF islets were enlarged with robust infiltration by CD68+ macrophages (**Fig. 3a**) of the M1 phenotype, as indicated by higher *Tnf* and *Nos2* and lower *Tgfb1*, *Il10* and *Arg1* expression in islets from ZDF compared to lean littermates (**Fig. 3b**). JD5037 treatment reduced macrophage infiltration and caused an M1-to-M2 shift (**Fig. 3a,b**). Islets from ZDF relative to lean littermates contained more Nlrp3, IL-1β (*Il1b*) and IL-18 (*Il18*) at both the mRNA and the protein levels, had more p65-NFκB protein and higher caspase-1 activity (**Fig. 3c**) and had similarly higher gene expression of the thioredoxin-interacting protein (*Txnip*)[34] and the IL-1 receptor (*Ilr1*) (**Fig. 3c**). In contrast, the same parameters in JD5037-treated ZDF rats were similar to or only slightly different from their levels in lean littermates, whereas expression of the IL-1R antagonist (*Il1rn*) was significantly higher (**Fig. 3c**).

The assembly of the functional inflammasome involves the interaction of the pyrin domains of Nlrp3 and the adaptor protein ASC[35]. Levels of the mRNA encoding ASC (*Pycard*) were higher in islets of ZDF rats compared to lean littermates and were normalized by JD5037 treatment. The expression of other inflammasomes, such as *Nlrp6*, *Nlrp12* and *Mnda*, was similar in lean and ZDF rats, and the slightly higher expression of *Aim2* in ZDF rats was unaffected by JD5037 treatment (**Supplementary Fig. 3a**). In islets from lean rats, both anandamide (l μM) and the positive control lipopolysaccha-ride (LPS) (10 ng ml^{-1}) increased ASC protein levels and the active, cleaved forms (p45 and p10) of caspase-1 (**Supplementary Fig. 3b**).

The anti-inflammatory function of adiponectin is well recognized[36], and its effects are mediated by Adiporl and Adipor2, both of which are abundantly expressed in islet beta cells[37]. Plasma concentrations of adiponectin (**Supplementary Table 1**) and levels of *Adiporl* and *Adipor2* mRNA in islets were lower in ZDF than in lean rats, whereas in JD5037-treated ZDF rats they were similar to those in lean controls (**Supplementary Fig. 3c**), Uric acid has been implicated in proinflammatory changes, decreased adiponectin production[38] and activation of the Nlrp3 inflammasome[39]. Plasma concentrations of uric

NIH-PA Author Manuscript

NIH-PA Author Manuscript

NIH-PA Author Manuscript

acid were higher in ZDF rats than in lean rats, whereas JD5037-treated ZDF rats had similar concentrations to those in lean littermates (**Supplementary Table 1**).

Both CB_1R and Nlrp3 were highly coexpressed with CD68 in pancreatic islets (72.3 ± 5.9% and 84.9 ± 9.8% colocalization, respectively), whereas tissue distribution of CB_1R and insulin did not overlap (5.4± 3.7% colocalization) (**Supplementary Fig. 4**).

Macrophage depletion delays the onset of T2DM

In ZDF rats treated with liposomes containing clodronate, a chemical agent inducing macrophage apoptosts[40], the onset of hyperglycemia and the progressive decline in plasma insulin and C-peptide were slower than in ZDF rats treated with empty liposomes, whereas both groups remained insulin resistant (**Fig. 4a**), similar to the insulin resistance of both vehicle-treated and JD5037-treated rats.

Macrophage infiltration of islets and expression of the macrophage-derived cytokines monocyte chemoattractant protein-1 (MCP-1) and TNF-α were lower in clodronate-treated than in empty liposome–treated ZDF rats (**Fig. 4b**). Pancreatic anandamide content, *Cnr1*, *Nlrfr3* and *Txnip* expression and Nlrp3 protein expression were similarly lower in clodronale-treated than in empty liposome-treated rats, which is compatible with infiltrating macrophages being their main source. Pancreatic insulin content was moderately higher in the former compared to the latter group (**Fig. 4b**).

Selective knockdown of macrophage CB_1R alleviates T2DM

We injected ZDF rats intraperitoneally (i.p.) daily with CB_1R siRNA delivery vehicles composed of βl,3-D-glucan–encapsulated siRNA particles (GeRPs) for 10 d to induce macrophage-specific knockdown of CB_1R (refs. 41,42). Controls received GeRPs containing scrambled siRNA. The siRNA selected for *in vivo* use produced dose-dependent, >95% suppression of CR_1R mRNA and no change in CR_2R mRNA in thiogtycollate-induced peritoneal elicited macrophages (PECs) (**Supplementary Fig. 5a**). We analyzed the selective uptake of GeRPs in peripheral blood leukocytes or PECs collected at the end of treatment and immunostained for CD68 and CD3 for FACS analysis. As previously reported[41], GeRPs were undetectable in peripheral blood monocytes (**Supplementary Fig. 5b**), whereas GeRPs were enriched approximately tenfold in $CD68^+$ PECs compared to $CD3^+$ lymphocytes (**Supplementary Fig. 5c**). Furthermore, in purified populations of peritoneal cells prepared by FACS, Cnrl was suppressed by 80% in $CD68^+FITC^+$ PECs (in which the glucan shell is labeled with F1TC) from ZDF rats treated with CB_1R GeRPs compared to those treated with scrambled GeRPs, with no change in *Cnr2* expression (**Supplementary Fig. 5d**). Neither *Cnr1* nor *Cnr2* expression was affected by CB_1R GeRP treatment in $CD3^+$ lymphocytes (**Supplementary Fig. 5e**).

ZDF rats treated with CR_1R siRNA remained normoglycemic and hyperinsulinemic, whereas those receiving scrambled siRNA developed progressive hyperglycemia and a decline in plasma insulin and C-peptide similarly lo vehicle-treated ZDF rats (**Fig. 5a**). CR_1R siRNA treatment also resulted in higher insulin expression and content in islets and lower macrophage infiltration and islet expression of *Nirp3*, *Pycard*, *Il1b*, *Il18*, Cnrl and

NIH-PA Author Manuscript

NIH-PA Author Manuscript

NIH-PA Author Manuscript

Ccl2 than did scrambled siRNA treatment (**Fig. 5b**). These effects were similar to those caused by JD5037 or clodronate treatment.

Glucose and palmitate boost macrophage anandamide levels

Islets isolated from ZDF rats had higher concentrations of anandamide, associated with lower activity of the enzyme that degrades it, fatty acid amide hydrolase (FAAH), and higher expression of its bio-synthetic enzyme, N-acyl phosphatidylethanolamine phospholipase D (NAPE-PLD), as compared to islets from lean rats or ZDF rats chronically treated with JD5037 (**Supplementary Fig. 6a**).

In contrast, concentrations of 2-arachidonoylglycerol (2-AG), the activity of the enzyme that degrades it, monoacylglyceride lipase, and the expression of its biosynthetic enzyme, diacylglycerol lipase-β (*Daglb*), were similar in the three groups, whereas *Dagla* expression was lower in islets from ZDF rats than in islets from lean litlermalcs (**Supplementary Fig, 6a**). NAPE-PLD was not coexpressed with insulin in islets (**Supplementary Fig. 6b**). Incubation of PECs from Jean rats with 250 μM palmitate or 33 mM glucose caused a modest or marked increase in anandamide levels, respectively, with the combination, of the two having an additive effect (**Supplementary Fig. 6c**).

Proinflammatory effect of anandamide is through macrophages

To further define the cells responsible for CR_1R-mediated proinflammatory signaling, we tested anandamide in RAW264.7 macrophages and M1N6 insulinoma cells, as well as in primary cultured human macrophages and PECs from wild-type, *Cnr1*$^{-/-}$ and *Nlrp3*$^{-/-}$ mice. In RAW264.7 cells, anandamide markedly increased the secretion of IL-1β, TNF-α and MCP-1, with peak changes observed at 0.5 μM, whereas it did not affect the much lower levels of these cytokines detectable in the medium of MIN6 cells relative to vehicle treatment (**Supplementary Fig.** 7a). Similarly, the expression of *Nlrp3*, *Casp1* and *Cnr1* was much higher in macrophages exposed lo anandamide compared to macrophages exposed to vehicle, whereas *Cnr2* expression was similar between the two groups. No differences in the expression of any of these genes were observed in MIN6 cells incubated with anandamide compared to vehicle (**Supplementary Fig. 7a**).

The above findings suggest that endocannabinoids induce beta cell apoptosis indirectly through macrophage-de rived cytokines, but they could also act directly on CB_1Rs present on beta cells[43]. We therefore compared the effects of maximally effective concentrations of anandamide and IL-1β on the gene expression of pro- and anti-apoptotic proteins and insulin in MIN6 cells (**Supplementary Fig. 7b**). Anandamide (10 μM) had liltle or no effecl on pro- and antiapoptotic gene expression, whereas Il-1β (30 ng ml^{-1}) markedly induced Ihe expression of Ihe proapoptolic genes *Bakl* and *Bax* and drastically suppressed the expression of the antiapoptotic genes *Bcl2* and *Bcl2l1*. IL-1β was similarly more potent than anandamide in influencing pro- and antiapoptolic gene expression in isolated human islets, indicating that effects seen in MIN6 cells are not unique to that tumor cell line (**Supplementary Fig. 7c**). IL-1β also drastically reduced the expression of *Cnr1* and CB_1R protein in MIN6 cells, and this effect was blocked by the IL-1R antagonist (**Supplementary Fig. 7d**).

NIH-PA Author Manuscript

NIH-PA Author Manuscript

NIH-PA Author Manuscript

We then analyzed the mechanism of the proinflammatory effect of anandamide in mouse PECs. Anandamide, relative to vehicle, induced proinflammatory gene expression in PECs from wild-type but not *Cnr1*$^{-/-}$ or *Nlrp3*$^{-/-}$ mice, whereas the expression of these genes was similarly higher in the presence of the LPS positive conlrol compared to vehicle in cells from wild-type and *Cnr1*$^{-/-}$ but not *Nlrp3*$^{-/-}$ mice (**Supplementary Fig. 8a,b**). This indicates the exclusive role of CB_1R and its downstream target Nlrp3 in mediating these effects. In agreement with earlier findings[14], acute *in vivo* treatment with anandamide (10 mg per kg body weight i.p.) induced whole-body insulin resistance in wild-type mice but failed to affect insulin-induced hypoglycemia in *Nlrp3*$^{-/-}$ mice, which, as reported by others[44], were supersensitive to insulin (**Supplementary Fig. 8c**).

There was also CB_1R-mediated inflammasome activation in human macrophages isolated from peripheral blood of 29 healthy subjects: *in vitro* incubation of such cells with anandamide resulted in higher *NLRP3*, *PYCARD*, *1L1B*, *IL18* and *CNR1* expression, lower *CNR2* expression and higher IL-1β and IL-18 secretion relative to that in vehicle-treated aliquots of the same cells, and no such differences were detectable in the added presence of 100 nM JD5037 (**Fig, 6a**).

We also assessed the effects of anandamide, IL-1β and high glucose in islets isolated from lean and ZDF rats (**Fig. 6b**). IL-1β secretion in aliquots of ten islets per replicate was higher in the presence than in the absence of either high glucose (33 mM) or anandamide (1 μM), with glucose being more effective than anandamide, and these differences were significantly greater in islets from ZDF compared to lean rats. 1L-1β (30 ng ml^{-1}), in turn, caused greater release of the chemokine MCP-1 and of IL-6 relative to vehicle, and this difference was amplified in ZDF islets, whereas high glucose had no such effect, and anandamide caused greater release than did vehicle of MCP-1 and IL-6 only in ZDF islets (**Fig. 6b**). None of these stimuli influenced TNF-α release. Finally, we replicated the greater effect of high glucose than anandamide on IL-1β release and IL-1β-induced MCP-1 release in normal human islets (**Fig. 6c**).

DISCUSSION

There is growing recognition that islet inflammation is involved in the progression of compensated insulin resistance to insulin-dependent T2DM, but the primary proinflammatory signal and its cellular target within the pancreatic islet have remained unidentified. Here we demon strate that endocannabinoids act in gthrough peripheral CB_1Rs mediate the progression of diabetes and the associated beta cell loss in a rat model of insulin-dependent T2DM. We further show that the CB_1Rs mediating these effects are located on infiltrating macrophages, where their activation induces the Nlrp3-ASC inflammasome and the proteolytic activation and release of IL-1β and IL-18, which act as paracrine signals to induce beta cell apoptosis.

The NOD-like receptors (NLRs) serve as intracellular platforms for the assembly of protein complexes or inflammasomes that coordinate inflammatory responses. Among the family of NLRs, the Nlrp3 inflammasome is unique in its ability to recognize molecular patterns associated with host-derived danger signals, such as certain mefabolites, and thus sense

NIH-PA Author Manuscript

NIH-PA Author Manuscript

NIH-PA Author Manuscript

metabolic stress. Indeed, increased expression and activity of the Nlrp3 inflammasome in the pancreas has been associated with beta cell death in a rodent model of DIO and T2DM[5,34]. Here we show that peripheral CB_1R blockade, compared with vehicle treatment, is associated with lower expression of Nlrp3 and the associated proteins Txnip and ASC in the islets of ZDF rats and delayed onset of markedly blunted hyperglycemia. This indicates that activation of CB_1Rs is the primary signal responsible for inflammasome activation and the resulting metabolic consequences. Metabolic factors known to activate Nlrp3 include K^+ efflux[45], reactive oxygen species[45] and a lowering of cAMP levels[46], and all three can be triggered by activation of G_i/G_o-coupled CB_1R (refs. 8,30). Another possible link is c-Jun N-terminal kinase (JNK), which is activated by CB_1R (ref. 47), and macrophage JNK is implicated in obesity-induced insulin resistance and inflammation[48]. Any or all of these mechanisms could contribute to the CB_1R-mediated increase in Nlrp3 expression.

Pancreatic beta cells express both endocannabinoids and CB_1R (refs. 43,49), and activation of CB_1R under *in vitro* conditions promotes apoptosis by inhibiting insulin signaling[27,13]. Additionally, the thioredoxin-interacting protein TXNIP, a signaling molecule that links endoplasmic reticulum stress to activation of the Nlrp3 inflammasome, has been linked to lipotoxic beta cell death through an autocrine mechanism documented under *in vitro* conditions[28,29]. Together, these findings could suggest that endocannabinoids induce beta cell death by acting directly on beta cells. Instead, we present four lines of evidence in support of an alternative, paracrine mechanism of beta cell death operating *in vivo* through activation of CB_1Rs on infiltrating macrophages to induce the production and release of proinflammatory cytokines, which then cause the apoptosis of neighboring beta cells.

First, CB_1R and Nlrp3 in the islets of diabetic ZDF rats colocalize with $CD68^+$ macrophages, but not with insulin-producing beta cells. Macrophages are known to express not only CB_1R[30], but also endocannabinoids[50], with both being upregulated under proinflammatory conditions[30,51], and stimulation of macrophage CB_1R increases the production of the chemokine MCP-l (ref. 30), which would promote transmigration of macrophages into islets. Accordingly, (he expression of *Ccl2* was higher in the pancreas of ZDF rats compared to lean controls and lower after JD5037 treatment.

Second, clodronate-induced depletion of macrophages or peripheral CB_1R blockade were associated with similarly slower and less severe progression of T2DM and the associated macrophage infiltration and Nlrp3 activation in pancreatic islets. The pancreatic expression of *Txnip* was also lower in clodronate-treated rats than in controls, indicating that it is triggered by infiltrating proinflammatory cells. This is further supported by the ability of IL-1β but not anandamide, to increase *Txnip* expression in beta cells *in vitro* and by the recent observation that endoplasmic reticulum stress causes a much more robust release of active IL-p in macrophages than in beta cells[29]. Furthermore, the findings that CB_1R agonists do not activate caspase or impair insulin release in cultured beta cells, whereas cytokines elicit their apoplosis[52], further support the dominance of a paracrine rather than autocrine mechanism of beta cell death.

Third, the endocannabinoid anandamidein duced the N1rp3 inflammasome and the inflammatory cascade it orchestrates *in vitro* in rodent and human macrophages, but not in

NIH-PA Author Manuscript

NIH-PA Author Manuscript

NIH-PA Author Manuscript

MIN6 insulinoma cells, and IL-1β robustly induced proapoptotic and suppressed anti-apoptotic gene expression in MIN6 cells. These effects maybe facilitated by the observed upregulation of IL-1β receptors in the pancreas in T2DM. At the same time, the gene expression of the 1L-1 receptor antagonist, a protein with therapeutic efficacy in T2DM[53], was higher in islets from JD5037-treated compared to vehicle-treated rats. The IL-1β–induced robust downregulation of *Cnr1* in MIN6 cells would further attenuate a direct effecl of anandamide on neighboring beta cells. The anandamide-induced 'autoinductton' of CB_1R expression in macrophages, also noted in other tissues[54], may represent a feed-forward mechanism whereby the initial CB_1R-mediated inflammatory signaling is amplified through upregulation of the receptor. Additionally, the exclusive role of CB_1R and Nlrp3 in mediating the proin flammatory effects of an an dam ide is indicated by the absence of these effects in macrophages from *Cnr1*$^{-/-}$ or *Nlrp3*$^{-/-}$ mice.

Fourth and most notably, selective *in vivo* knockdown of macrophage CB_1R fully replicates the effect of pharmacological CB_1R blockade in restoring normoglycemia by protecting and restoring beta cell functions. Selective knockdown of macrophage CB_1R also prevented macrophage infiltration of the islets and the increases in pancreatic anandamide, CB_1R, MCP-1, Nlrp3 and Il-1β, as compared to scrambled siRNA-treated controls, This indicates that activation of macrophage CB_1Rs by endogenous anandamide is not only the signal for inflammasome activation but also a trigger for the production of the chemokine that promotes the transmigration of macrophages into the pancreas.

Of the two main endocannabinoids, anandamide levels are higher in the islets of ZDF compared to those of lean rats as a result ofboth its increased biosynthesis and decreased degradation by FAAH in the former, whereas 2-AG levels remain similar in the two groups. High glucose and palmitate levels may be the triggers for the diabetes-related increase in anandamide in proinflammatory macrophages. The diabetogenic role of anandamide is supported by the finding that chronic anandamide treatment of lean mice induces glucose intolerance and muscle macrophage infiltration[55], further, the selective increase in plasma anandamide, but not 2-AG, correlates with increased body mass and proinflammatory metabolite levels in subjects with diabetes[56], though others have reported higher concentrations of both endocannabinoids in subjects with diabetes compared to healthy subjects[15].

Beta cell survival may be improved indirectly through reversal of insulin resistance. However, this is not the mechanism of the improved beta cell function in JD5037-treated ZDF rats, which remained insulin resistant. This unexpected finding is probably related to the paradoxical increase in the hyperinsulinemia resulting from the improved beta cell survival in JD5037-trealed ZDF rats, as hyperinsulinemia can drive, rather than simply compensate for, insulin resistance[57]. Conditions are different in insulin-resistant DIO mice, in which beta cell function is not compromised and CB_1R blockade has been found to reverse both hyperinsulinemia and insulin resistance[22,23]. The CB_1R-mediated insulin resistance in these models may also involve inflammasome activation, as suggested by our finding that anandamide induced insulin resistance in wild-type but not *Nlp3*$^{-/-}$ mice.

NIH-PA Author Manuscript

NIH-PA Author Manuscript

NIH-PA Author Manuscript

Beta cell apoptosis may also be secondary to hypothalamic inflammation[32]. However, such a central mechanism is an unlikely target or JD5037 because the low brain penetrance of the compound does not lead to significant brain CB_1R occupancy[23]. Also, selective down regulation of peripheral CB_1R levels by CB_1R antisense oligonucleotides is associated with improved metabolic profile in AKR mice with DIO[58]. Although we cannot absolutely rule out off-target effects of JD5037, a possible non-CB_1R target for JD5037 or one of its metabolites is unlikely in view of the lack of a tit idi abet ic effects of its CB_1R-inactive diastereomer.

The dominant role of macrophages in progressive beta cell death, as indicated here, does not exclude the possible role of beta cells in initiating diabetic insulitis through glucose-induced IL-1β release[59], which stimulates secretion of the chemokine MCP-1. MCP-1 promotes macrophage infiltration, which then drives progressive islet inflammation and beta cell death. The pathogenic role of infiltrating macrophages may also apply to human T2DM: macrophages isolated from individuals with diabetes express more *Nlrp3* and secrete more IL-1β than macrophages from healthy controls[7], and these changes are probably triggered by endocatmabinoid activation of CB_1R, as indicated by the present findings. Macrophages also express CR_2R, whose stimulation suppresses proinflammatory cytokine production[60]. It remains to be seen whether selective CR_2R agonists may also be effective in protecting beta cells in T2DM.

In summary, we provide multiple lines ofevidence for the key role of macrophage-derived anandamide in beta cell loss in T2DM, as illustrated schematically in **Figure 6d**, and identify CB_1R on macrophages as a new therapeutic target.

ONLINE METHODS

Animals

Animal protocols were approved by the Institutional Animal Care and Use Committee of the NIAAA, NIH. Male ZDF rats with their lean controls were obtained from Charles River Laboratories (Wilmington, MA, USA). *Cnr1*$^{-/-}$ and wild-type littermate mice backcrossed to a C57BL/6 background were bred as described earlier*61*. *Nlrp3*$^{-/-}$ and wild-type littermate mice on a mixed C57BL/6J-C57BL/6N background were purchased from The lackson Laboratory (Bar Harbor, ME, USA). Animals were individually housed and maintained under a 12-h light-dark cycle and fed *ad libitum* with a standard laboratory diet (STD, NIH-31 rodent diet).

ZDF rats received JD5037 or vehicle (4% DMSO + 1% Tween 80 in PBS) by oral gavage according to two different protocols. In the first one, 8-week-old diabetic ZDF rats were given 3 mg per kg body weight per day JD5037 or vehicle for 28 d, with lean controls receiving vehicle only. In the second protocol, similar treatment was started In 6-week-old predlabetlc ZDF rats and age-matched lean controls, and treatment continued for 12 weeks until the age of 18 weeks. Body weight and food intake were monitored dally. Blood glucose was monitored weekly, and plasma insulin and C-peptide concentrations were determined every 4 weeks. At the end of treatment in both protocols, rats were decapitated, the brain, liver, kidney, pancreas and combined fat pads were removed, weighed, and snap-frown in

NIH-PA Author Manuscript

NIH-PA Author Manuscript

NIH-PA Author Manuscript

liquid nitrogen or fixed in formalin, and trunk blood was collected for determining endocrine and biochemical parameters. Adiposity Index was defined as the combined weight of the epidydlinal, retroperitoneal and inguinal fat pads, expressed as percentage of total body weight.

Peripheral CB_1 receptor antagonist

JDS037 and Its inactive diastereomer ID50371 were synthesized and their pharmacological properties analyzed as described earlier[23,62].

Blood chemistry

Blood glucose levels were determined using the Elite gluco-meter (Bayer, Pittsburgh, PA). Serum alanine aminotransferase (ALT), total cholesterol and triglyceride levels were quantified by colorlmetric kits from BioAssay Systems. Plasma Insulin was measured using the Ultra Sensitive Rat insulin ELISA Kit (Crystal Chem). Hemoglobin Ale was determined using the Rat Hemoglobin Ale (HbA1c) Assay Kit (Crystal Chem), and C-peptlde was quantified by ELISA (Rat C-peptide ELISA, ALPCO). Serum leptin and adi-ponectin we re deter mined by ELISA (B-Bridge International), α-amylase, lipase and uric acid concentrations were determined using commercially available colorimetric kits (BioAssay Systems). TNF-α and TL-1β concentrations were determined using TNF-α ELISA Kit (For Lysates) (RayBlotech) and IL-1β Rat ELISA Kit (Abeam), respectively.

Liver parameters

To determine intrahepatic triglyceride and cholesterol content, liver tissue was extracted as described previously[63]. After extraction, 0.5 ml of organic phase was transferred to a clean tube containing 1 ml of 2% Triton X-100 in chloroform and dried under a stream of nitrogen, The residue was resolublllzed in 1 ml of distilled water, and triglyceride content was determined using EnzyChrom Triglyceride Assay Kit.

Enzyme and edocannabinoid measurements

Fatty acid amide hydrolase (FAAH) and monoacylglycerlde lipase (MAGL) activity in homogenates of isolated pancreatic islets was measured as previously described[64], using 25 μg of protein for FAAH activity and 15 μg for MAGL to compensate for the higher MAGL expression In Islets. Tissue extraction and measurement of anandamide by liquid chromatography–tandem mass spectrometry (LC-MS/MS) was performed as described previously[65].

Hyperinsufineinic-eugfycemic clamp

Clamps and glucose tracer analyses in conscious rats were performed as follows: the right jugular vein of three rats per group was catheterlzed a week before the experiment; the rats were allowed to recover; and clamps were performed by continuous infusion of Insulin at 3 mU per kg body weight per mln and co-Infusion of glucose to maintain euglycemia. The protocol for radioactive clamps to evaluate glucose fluxes was adapted from Buettner *et al*[66]. ^{3}H-D-Glucose (PerkinElmer) was first Infused at 0.8 μCl/min for 1 mln and then at 0.04 μCI/min for 2 h before insulin Infusion. The tritiated glucose infusion was pursued

NIH-PA Author Manuscript

NIH-PA Author Manuscript

NIH-PA Author Manuscript

during the rest of the experiment at the same rate. We sampled 10 µ1 of blood from the tall at 15 and 5 mln before starting insulin Infusion and at 30, 20, and 10 min before the end of the experiment under steady-state conditions.

Blood samples were centrlfuged and the serum was snap-frozen on dry ice. Once all the samples were available, 5 µ1 serum was transferred to 25 µl deion-Ized water and then mixed with 25 µl of 0.1 N $ZnSO_4$. Samples were precipitated by the addition of 25 µl of 0.1 N $Ba(OH)_2$. After centrifugatlon, the supernatant was dried overnight and resuspended in water, and radioactivity was determined by liquid scintillation spectrometry. Glucose turnover was calculated as the ratio of tritiated glucose infusion rate over the specific activity of blood glucose.

Isolation of pancreatic islets and measurement of insulin secretion

Rats were fasted for 12 h, and tail blood was collected to determine basal insulin and C-peptlde levels. Rats were then given glucose (3 g per kg body weight) orally by gavage, and 5 min later tail blood was again collected for determining insulin and C-pept Ide con centratlons, w 1th the dlffe rence ove r basel ine values considered as a measure of glucose-induced insulin and C-peptide release, with the latter used to assess the role of insulin production compared to clearance In the observed change in piasma insulin concentrations.

After 4 d of recovery, pancreata from treated animals were inflated through the common bile duct with a solution of Llberase TL Research Grade (1.18 U/ml, Roche Diagnostics) and digested for 30 mln at 37 °C. Islets were purified on a discontinuous Flcoll gradient (GE Healthcare) and handplcked under a stereomlcroscope for immediate assessment of beta cell function by static Incubation. Right after isolation, batches of four Islets were preincubated for 2 h in RPMI 1640 containing NaHOO, (2 g/1), HEPES (25 mM), 10% (v/v) neonatal calf serum (Invltrogen) (pH 7.2) and 0.5 g/l glucose at 37 °C In an Incubator under an atmosphere of 5% C02. This was followed by successive 1-h incubations In the presence of 0.5,1, 1.5,2 and 3 g/1 glucose. Supernatants were collected in each step for insulin quantification (Crystal Chem). For each condition, the experiments were performed in triplicate of five islets from five biological replicates.

Depletion of pancreatic macrophages with clodronate-containing liposomes

Clodronate-containing liposomes were prepared as described[67]. Briefly, phosphatidylcholine (86 mg) and 8 mg cholesterol were dissolved in 10 ml of chloroform in a 500-ml round-bottom flask. Chloroform was removed by low- vacuum rotary evaporation at 37 °C. The thin film that formed on the walls of the flask was dispersed by gentle shaking for 10 min in 10 ml of PBS or 0.6 M clodronate dissolved in PBS. The suspensions were kept under argon for 2 h at room temperature, sonicated for 3 min In a water bath sonlcator and kept under argon for another 2 h. The nonencapsulated clodronate was removed by centrifugatlon (10,000g for 15 mln) of the liposomes. The white band at the top of the suspension, which contained clodronate-containing liposomes, was retrieved and washed twice with PBS (sterilized) by centrifugation (25,000g for 30 min). Finally, the pellet was resuspended In 4 ml of sterilized PBS and stored at 4 °C for up to 1 month before use. Rats were injected i.p. with clodronate-containing liposomes (1 ml) three times at 3-d intervals between two

NIH-PA Author Manuscript

NIH-PA Author Manuscript

NIH-PA Author Manuscript

consecutive injections. Glycemia was monitored every 4 d as previously described. Twenty days after the first injection, rats were killed and tissues collected The pancreas was fixed in 10% neutral buffered formalin (NBF), embedded In paraffin and sectioned (4 μm) onto glass slides, Specific staining was performed as described below.

Preparation of peritoneal macrophages and siRNA-niediated gene silencing

Eight-week-old ZDF rats were Injected i.p. with 4% thioglycollate broth (Sigma-Aldrich). Five days later, the peritoneal cavity was washed with PBS, and peritoneal fluid was collected, filtered through a 70-μm-pore-dlameter nylon mesh and centrifuged. The pellet was first treated with red blood cell lysis buffer and plated in DMEM supplemented with 10% FBS, 50 μg/ml streptomycin and 50 U/ml of penicillin. Twenty-four hours later, aliquots of 1×10^6 peritoneal elicited cells (PECs) were treated with 80, 160 or 240 pmol of scrambled or *Cnr1* siRNA (Dharmacon) or with 3 nmol Endo-Porter in PBS. Twenty-four hours later, mRNA was extracted and reverse transcribed to measure the level of *Cnr1* mRNA by qPCR. The siRNA species producing the greatest degree of knockdown was then used to prepare GeRPs, as described below.

Preparation and in vivo administration of glucan-encapsulated siRNA particles

FITC-labeled glucan shells were prepared as previously described[68]. To prepare a glucan-encapsulated stRNA particle (GeRP) dose for one rat, 30 nmol slRNA (Dharmacon) were Incubated with 500 nmol Endo-Porter (Gene Tools) In 30 mM sodium acetate (pH 4.8) for 15 mln at room temperature in a final volume of 200 μl. The sIRNA–Endo-Porter solution was added to 10 nig (~ 10^{10} particles) of FITC-glucan shells and then vortexed and incubated for 1 h. The siRNA- loaded GeRPs were then resuspended in 5 ml PBS and sonicated to ensure homogeneity of the GeRP preparation.

Twelve 8-week old ZDF rats were then injected i.p. once daily for 10 d with 5.6 mg per kg body weight GeRPs loaded with 2.1 ing per kg body weight EP and 0.262 mg per kg body weight siRNA. Six rats were then treated with a scrambled siRNA (sense CAGUCGCGUUUGCGACUGGUU, antisense CCAGUCG-CAAACGCGACUGUU), and six other rats received an siRNA directed against *Cnr1* (sense GCAUCAAGAGCACCGUUAAUU, antisense UAACGGUGCUCUUGAUG-CUU).

Cell preparation and FACS analysis of $CD3^+$ and $CD68^+$ cells from blood or peritoneal cavity

FACS analyses were performed to determine uptake of GeRP by macrophages compared to lymphocytes and to estimate the proportion of $CD68^+$and $CD3^+$ cells in the white blood cell fraction or in the peritoneal lavage fluid of the GeRP-treated ZDF rats. PECs were prepared as described previously, and the white blood cell fraction was prepared by adding 250 μL of whole blood into a red blood cell lysis buffer for 5 min and centrifuging at 500g for 10 min. The resulting pellets were washed in PBS containing 294 FBS, and cells were then preincubated with Rat BD Fc Block (purified mouse antl-rat CD32, BD Biosciences 550270, San Diego, CA, 1: 100) at 4 °C for 10 min and then stained for CD3 (mouse anti-rat CD3, Alexa Fluor 647; MCA772A647, AbD serotec, 1:10) or CD68 (mouse antl-rat CD6S, Alexa Fluor 647; MCA341A647, AbD serotec, 1:10) for 30 min at 4 °C Flow cytometry analysts

NIH-PA Author Manuscript

NIH-PA Author Manuscript

NIH-PA Author Manuscript

was performed using a FACSCalibur (BD Biosciences), and quantification of $CD3^+$ and$CD68^+$ cells was achieved using Flowjo software. To assess $CD68^+$ cell-specific and selective knockdown of CB_1R, we stained PECs with a mouse anti-rat CD3 antibody conjugated to allophycocyanin and a mouse anti-rat CD68 antibody conjugated to phycoerythrin (MCA772A647 and MCA341PE, respectively, AbD Serotec, 1:10). Cells were then maintained In PBS supplemented with 2% FBS and were sorted using a BD FACS Aria. After sorting, the two populations were analyzed separately for *Cttr1* and *Cnr2* mRNA expression.

Pancreas immunohistology

Pancreas was fixed in 10% neutral buffered formalin (NBF), embedded in paraffin and sectioned (4 μm) onto glass slides. Antibodies used for Immunostaining are listed in **Supplementary Table 2.** Each bound antibody was revealed using the appropriate Elite ABC horseradish peroxidase (HRP)-diaminobenzediene (DAB) system (Vector Labs). To determine whether any colocalization was occurring, we used the same pairs of antibodies listed in **Supplementary Table 2.** For detection, secondary antibody coupled to FITC or phycoerythrin was used. Images were viewed with a Fluoview FVI01 confocal microscope system (Olympus), Images were then analyzed using ImageJ software, and the presence or absence of colocalization was assessed by calculating the Pearson's coefficient.

TUNEL staining was performed using the TUNEL Apoptosis Detection Kit (GenScrlpt USA). Sections were then counterstalned with hematoxylin, Gill's formula (Vector Labs) and analyzed using an Olympus BX41 microscope.

Beta cell mass

Beta cell mass was evaluated by point counting morphometry on insulin antibody-stained sections of pancreas as previously described[69]. Briefly, multiple sections (separated by 80 μm each) from each pancreas were analyzed systematically by using a grid system covering at least 175 fields per rat. Separate images were acquired with a BX41 microscope (Olympus), and relative volumes were calculated for beta cells, non-beta cells and exocrine tissue using ImageJ software. The extent of contaminating tissue (for example, pancreatic ducts, adipose tissue and so on) was recorded In order to correct for the pancreatic weight, Beta cell mass was calculated using the following formula: islet beta cell mass = relative beta cell volume × corrected pancreatic weight.

Inflammasome characterization

Active form of p65-NF-κB was detected using the TransAM NF-κB Transcription Factor ELISA Kit (Active Motif), caspase-1 activity was determined using the Caspase-1 Assay Kit (Fluorometric) from Abeam (ab39412), IL-1β abundance was measured using the IL-1β Rat ELISA Kit (Abeam) and IL-18 abundance with the IL-18 Rat ELISA Kit (Life Technologies).

Cell culture and extraction

Mouse RAW264.7 macrophages (American Type Culture Collection, Manassas, VA) were cultured as previously described[70] and incubated for 4 h with various concentrations of

NIH-PA Author Manuscript

NIH-PA Author Manuscript

NIH-PA Author Manuscript

anandamide (0.1, 0.5, 1 and 10 μM) In the absence or presence of JD5037 (100 nM). Mouse MIN6 insulinoma cells were a gift from NIDDK and were cultured In low-glucose DMEM (Gibco 11885) supplemented with 15% FBS (BenchMark 100-006) and 1% antibiotic-antlmycotlc cocktail (Invltrogen 15240-096). Cells were either treated for 4 h with various concentrations of anandamide (0.5,1 and 5 μM) or with 30 ng/ml of IL-1β (Abeam Ab9723).

PECs were prepared as described above and plated for 24 h and then incubated in DMEM supplemented with 10% FBS, 50 μg/ml streptomycin and 50 U/ml penicillin supplemented with palmitic acid (250 μM) or glucose (33.3 mM final) for 24 h.

Pancreatic islets from lean and ZDF rats were isolated as previously described. HuMan islets (Caucasian female donor) were purchased from Lonza (201985). Ten rat Islets per replicate were incubated for 24 h at 37 °C in DMEM (5.5 mM glucose) containing 10% FBS, 50 μg/ml streptomycin and 50 U/ml penicillin, supplemented either with anandamide (1 μM), IL-1β (30 ng/ml) or glucose (33.3 mM). Human islets were maintained in culture according to guidelines from the commercial source and were treated the same way as rat islets.

For all cell types, mediuM was collected and immediately frozen In liquid nitrogen. Cells were washed twice In ice-cold sterile PBS before harvesting. Endocannabinold levels were determined as previously described, and secretion of IL-1β, IL-18, TNF-α and MCP-1 in the medium from RAW264.7 and MIN6 cells was determined using ELISA kits (Biosensls BEK-2151-2P, Uscn Life Science & Technology Company E90064Mu, Biosensis BEK-2102-2P, Uscn Life Science & Technology Company E90087Mu, respectively). IL-1β IL-6, TNF-α and MCP-1 secretion from rat islets was determined using ELISA kits from Abeam and Life Technologies (Abi00768,KRC006i,KRC3011 and KRC1011, respectively). Human islet secretion of IL-1β was assessed using the ELISA kit from Life Technologies (KHC0011), and MCP-1 was evaluated using ELISA kit from R&D Systems (DCP00).

Human monocyte-derived macrophages

Peripheral blood mononuclear cells (PBMCs) were freshly isolated from heparinized venous blood drawn from healthy volunteers using Histopaque –1077 solution (Sigma), as described previously[71]. The protocol was approved by the Institutional Review Board of the National Institute of Diabetes, Digestive and Kidney Diseases (NIDDK), National Institutes of Health (NIH), and all subjects had given informed consent. Adherent monocyte subpopulations were collected from PBMCs, and monocyte-derived macrophages (MDM,) were prepared by culturing peripheral blood monocytes for 5 d in the presence of 2 ng/ml of human macrophage colony-stimulating factor (Sigma, St. Louis, MO). Cells were cultured in complete RPMI 1640 medium (Glbco-BRL, Grand Island, NY) with 10% heat-in activated FBS. MDMs were then exposed to vehicle, anandamide (0.5 μM), JD5D37 (100 nM) or their combination for 24 h. Culture medium was collected for cytokine measurement (IL-1β Human ELISA Kit ab46052 from Abeam and Human Interleukin 18 Kit BEK-2119-2P from Biosensls), and cells were washed with ice-cold PBS before RNA extraction.

Western blotting

CB_1R relative protein content was assessed by western blotting using a CB_1R polyclonal antibody diluted 1:1,000 (Cayman, 101500). Caspase-1 processing was evaluated using an

NIH-PA Author Manuscript

NIH-PA Author Manuscript

NIH-PA Author Manuscript

antl-caspase-1 polyclonal antibody diluted 1:1,000 (Santa Cruz Biotechnology, sc-514), ASC was assessed using anti-TMS1 polyclonal antibody diluted 1:500 (Cell Signaling, 4628), and β-actin was evaluated using an anti-β-actin antibody coupled to horseradish peroxidase (Abeam, ab49900). Blots were revealed using SuperSignal WestPico Chemiluminescence (Thermo Scientific), and quantification was performed using the gel analysis options of ImageJ software.

RT-PCR

Total mRNA from pancreatic Islets, RAW264.7 cells, MIN6 cells, PECs and human MDMs were extracted using Qiagen RNeasy Mini Kit (74104). All extractions were followed by DNase I treatment (Invitrogen). Total mRNA was reverse transcribed using the iscript cDNA kit (Elo-Rad). RT-PCR was performed as described previously[17] in a 96-well plate using a StepOne Plus Real-Time PCR system (Applied Blosystems). QuantiTect Primer Assays were used to detect gene expression (**Supplementary Table 3**). Expression of the gene of interest is given as a relative value comparing it to the geometric average of *18S*, *L19*, *L38* and TATA box binding protein (*Tbp*) mRNA expression.

Statistical analyses

Values are expressed as means ± s.e.m. Data were subjected to one-way analysis of variance (ANOVA), followed by the Tukey-Kramer *post hoc* test. Time-dependent variables were analyzed and results in multiple groups were compared by ANOVA followed by Bonferroni test. (GraphPad Prism 6 for Windows). Significance was set at $P < 0.05$.

Acknowledgments

We thank J.F. McElroy and R.J. Chorval (Jenrin Discovery) for providing the CB_1R antagonist JD5037 and its inactive diastereomer. O. Gavrilova (NIDDK, US National Institutes of Health (NIH)) for advice on pancreatic islet isolation, J. Harvey-While for technical assistance, D. Feng for FACS analyses, R. Kechrid for assistance with the animal studies and P. Staker for collecting human blood specimens, This study was supported by intramural NIH funds, The work from M.P.C.'s laboratory was supported by grants from the NIH (DK0857S3 and A1046629).

References

1. Defronzo RA. Banting Lecture. From the triumvirate to the ominous octet: a new paradigm for the treatment of type 2 diabetes mellitus. Diabetes. 2009; 58:773–795. [PubMed: 19336687]
2. Shoelson SE, Lee J, Goldline AB. Inflammation and insulin resistance. J. Clin. invest. 2006; 116:1793–1801. [PubMed: 16823477]
3. Ehses JA, et al. Increased number ot islet-associated macrophages in type 2 diabetes. Diabetes. 2007; 56:2356–2370. [PubMed: 17579207]
4. Masters SL, et al. Activation of the NLRP3 inflammasome by islet amyloid polypeptide provides a mechanism for enhanced IL-1β in type 2 diabetes. Nat. Immunol. 2010; 11:897–904. [PubMed: 20835230]
5. Youm YH, et al. Elimination of the NLRP3-ASC inflammasorne protects against chronic obesity-induced pancreatic damage. Endocrinology. 2011; 152:4039–4045. [PubMed: 21862613]
6. Goossens GH, et al. Expression of NLRP3 inflammasome and T cell population markers in adipose tissue are associated with insulin resistance and impaired glucose metabolism in humans. Mol. Immunol. 2012; 50:142–149. [PubMed: 22325453]
7. Lee HM, et al. Upregulatcd NLRP3 inflammasome activation in patients with type 2 diabetes. Diabetes. 2013; 62:194–204. [PubMed: 23086037]

NIH-PA Author Manuscript

NIH-PA Author Manuscript

NIH-PA Author Manuscript

8. Pacher P, Batkai S, Kunos G. The endocannabinoid system as an emerging target of pharmacotherapy. Pharmacol, Rev. 2006; 58:389–462. [PubMed: 16968947]
9. Di Marzo V, et al. Leptin-regulated endocannabinoids are involved in maintaining food intake. Nature. 2001; 410:822–825. [PubMed: 11298451]
10. Cota D, et al. The endogenous cannabinoid system affects energy balance via central orexigenic drive and peripheral lipogenesis. J. Clin. Invest. 2003; 112:423–431. [PubMed: 12897210]
11. Osei-Hyiaman D, et al. Endocannabinoid activation at hepatic CB1 receptors stimulates fatty acid synthesis and contributes to diet-induced obesity. J. Clin. Invest. 2005; 115:1298–1305. [PubMed: 15864349]
12. Jourdan T, et al. Antagonism of peripheral hepatic cannabinoid receptor-1 improves liver lipid metabolism in mice: evidence from cultured esplants. Hepatology. 2012; 55:790–799. [PubMed: 21987372]
13. Eckardt K, et al. Cannabinoid type I receptors in human skeletal muscle cells participate in the negative crosstalk between fat and muscle. Diabetologia. 2009; 52:664–674. [PubMed: 19089403]
14. Liu J, et al. Hepatic cannabinoid receptor-1 mediates diet-induced insulin resistance via inhibition ol insulin signaling and clearance in mice. Gastroenterology. 2012; 142:1218–1228. [PubMed: 22307032]
15. Matias I, et al. Regulation, function, and dysregulation of endocannabinoids in models of adipose and beta-pancreatic cells and in obesity and hyperglycemia. J. Clin. Endocrinol. Metab. 2006; 91:3171–3180. [PubMed: 16684820]
16. Ravinet Trillou C, et al. Anti-obesity effect of SR14716, a CB1 receptor antagonist, in diet-induced obese mice. Am. J. Physiol. Regul. Integr. Comp. Physiol. 2003; 284:R345–R353. [PubMed: 12399252]
17. Jourdan T, et al. CB1 antagonism exerts specific molecular effects on visceral and subcutaneous fat and reverses liver steatosis in diet-induced obese mice. Diabetes. 2010; 59:926–934. [PubMed: 20110567]
18. Després JP, Golay A, Sjostrom L. Effects of rimonabant on metabolic risk factors in overweight patients with dyslipidemia. N. Engl. J. Med. 2005; 353:2121–2134. [PubMed: 16291982]
19. Addy C, et al. The acyclic CB1R inverse agonist taranabant mediates weight loss by increasing energy expenditure and decreasing caloric intake. Cell Metab. 2008; 7:68–78. [PubMed: 18177726]
20. Rosenstock J, Hollander P, Chevalier S, Iranmanesh A. SERENADE: the Study Evaluating Rimonabant Efficacy in Drug-naive Diabetic Patients: effects of monotherapy with rimonabant, the first selective CB1 receptor antagonist, on glycemic control, body weight, and lipid profile in drug-naive type 2 diabetes. Diabetes Care. 20O8; 31:2169–2176. [PubMed: 18678611]
21. Le Foll B, Gorelick DA, Goldberg SR. The future of endocannabinoid-oriented clinical research after CB1 antagonists. Psychopharmacology (Berl.). 2009; 205:171–174. [PubMed: 19300982]
22. Tam J, et al. Peripheral CB1 cannabinoid receptor blockade improvescardiometabolic risk in mouse models of obesity. J. Clin. Invest. 2010; 120:2953–2966. [PubMed: 20664173]
23. Tam J, et al. Peripheral cannabinoid-1 receptor inverse agonism reduces obesity by reversing leptin resistance. Cell Metab. 2012; 16:167–179. [PubMed: 22841573]
24. Jetton TL, et al. Mechanisms of compensatory beta-cell growth in insulin-resistant rats: roles of Akt kinase. Diabetes. 2005; 54:2294–2304. [PubMed: 16046294]
25. Topp BG, Atkinson LL, Finegood DT. Dynamics of insulin sensitivity, -cell function, and -cell mass during the development of diabetes in fa/fa rats. Am. J. Physiol. Endocrinol. Metab. 2007; 293:E1730–E1735. [PubMed: 17895283]
26. Rohrbach K, et al. Ibipinabant attenuates beta-cell loss in male Zucker diabetic fatty rats independently of its effects on body weight. Diabetes Obes. Metab. 2012; 14:555–564. [PubMed: 22268426]
27. Kim W, et al. Cannabinoids induce pancreatic beta-cell death by directly inhibiting insulin receptor activation. Sci. Signal. 2012; 5:ra23. [PubMed: 22434934]
28. Oslowski CM, et al. Thioredoxin-interacting protein mediates ER stress-induced beta cell death through initiation of the inflammasome. Cell Metab. 2012; 16:265–273. [PubMed: 22883234]

NIH-PA Author Manuscript

NIH-PA Author Manuscript

NIH-PA Author Manuscript

29. Lerner AG, et al. IRE1alpha induces thioredoxin-interacting protein to activate the NLRP3 inflammasome and promote programmed cell death under irremediable ER stress. Cell Metab. 2012; 16:250–264. [PubMed: 22883233]
30. Han KH, et al. CB1 and CB2 cannabinoid receptors differentially regulate the production of reactive oxygen species by macrophages. Cardiovasc. Res. 2009; 84:378–386. [PubMed: 19596672]
31. Osundiji MA, et al. Brain glucose sensors play a significant role in the regulation of pancreatic glucose-stimulated insulin secretion. Diabetes. 2012; 61:321–328. [PubMed: 22210318]
32. Calegari VC, et al. Inflammation of the hypothalamus leads to defective pancreatic islet function. J. Biol. Chem. 2011; 286:12870–12880. [PubMed: 21257748]
33. O'Hare JD, Zielinski E, Cheng B, Scherer T, Buettner C. Central endocannabinoid signaling regulates hepatic glucose production and systemic lipolysis. Diabetes. 2011; 60:1055–1062. [PubMed: 21447652]
34. Zhou R, Tardivel A, Thorens B, Choi I, Tschopp J. Thioredoxin-interacting protein links oxidative stress to inflammasome activation. Nat. Immunol. 2010; 11:136–140. [PubMed: 20023662]
35. Schroder K, Tschopp J. The inflammasomes. Cell. 2010; 140:821–832. [PubMed: 20303873]
36. Wolf AM, Wolf D, Rumpold H, Enrich B, Tilg H. Adiponectin induces the anti-inflammatory cytokines IL-10 and IL-1RA in human leukocytes. Biochem. Biophys. Res. Commun. 2004; 323:630–635. [PubMed: 15369797]
37. Kharroubi I, Rasschaert J, Eizirik DL, Cnop M. Expression of adiponectin receptors in pancreatic beta cells. Biochem. Biophys. Res. Commun. 2003; 312:1118–1122. [PubMed: 14651988]
38. Baldwin W, et al. Hyperuricemia as a mediator of the proinflammatory endocrine imbalance in the adipose tissue in a murine model of the metabolic syndrome. Diabetes. 2011; 60:1258–1269. [PubMed: 21346177]
39. Martinon F, Petrilli V, Mayor A, Tardivel A, Tschopp J. Gout-associated uric acid crystals activate the NALP3 inflammasome. Nature. 2006; 440:237–241. [PubMed: 16407889]
40. van Rooijen N, Hendrikx E. Liposomes for specific depletion of macrophages from organs and tissues. Methods Mol. Biol. 2010; 605:189–203. [PubMed: 20072882]
41. Aouadi M, et al. Orally delivered siRNA targeting macrophage Map4k4 suppresses systemic inflammation. Nature. 2009; 458:1180–1184. [PubMed: 19407801]
42. Tesz GJ, et al. Glucan particles for selective delivery of siRNA to phagocytic cells in mice. Biochem. J. 2011; 436:351–362. [PubMed: 21418037]
43. Kim W, et al. Cannabinoids inhibit insulin receptor signaling in pancreatic beta-cells. Diabetes. 2011; 60:1198–1209. [PubMed: 21346174]
44. Stienstra R, et al. The inflammasome-mediated caspase-1 activation controls adipocyte differentiation and insulin sensitivity. Cell Metab. 2010; 12:593–605. [PubMed: 21109192]
45. Dostert C, et al. Innate immune activation through Nalp3 inflammasome sensing of asbestos and silica. Science. 2008; 320:674–677. [PubMed: 18403674]
46. Lee GS, et al. The calcium-sensing receptor regulates the NLRP3 inflammasome through Ca^{2+} and cAMP. Nature. 2012; 492:123–127. [PubMed: 23143333]
47. Liu J, et al. Functional CB1 cannabinoid receptors in human vascular endothelial cells. Biochem. J. 2000; 346:835–840. [PubMed: 10698714]
48. Han MS, et al. JNK expression by macrophages promotes obesity-induced insulin resistance and inflammation. Science. 2013; 339:218–222. [PubMed: 23223452]
49. Starowicz KM, et al. Endocannabinoid dysregulation in the pancreas and adipose tissue of mice fed with a high-fat diet. Obesity (Silver Spring). 2008; 16:553–565. [PubMed: 18239598]
50. Di Marzo V, De Petrocellis L, Sepe N, Buono A. Biosynthesis of anandamide and related acylethanolamides in mouse J774 macrophages and N18 neuroblastoma cells. Biochem. J. 1996; 316:977–984. [PubMed: 8670178]
51. Varga K, Wagner JA, Bridgen DT, Kunos G. Platelet- and macrophage-derived endogenous cannabinoids are involved in endotoxin-induced hypotension. FASEB J. 1998; 12:1035–1044. [PubMed: 9707176]

NIH-PA Author Manuscript

NIH-PA Author Manuscript

NIH-PA Author Manuscript

52. Vilches-Flores A, Hauge-Evans AC, Jones PM, Persaud SJ. Chronic activation of cannabinoid receptors in vitro does not compromise mouse islet function. Clin. Sci. (Lond.). 2013; 127:467–478. [PubMed: 23078523]
53. Larsen CM, et al. Interleukin-1-receptor antagonist in type 2 diabetes mellitus. N. Engl. J. Med. 2007; 356:1517–1526. [PubMed: 17429083]
54. Mukhopadhyay B, et al. Transcriptional regulation of cannabinoid receptor-1 expression in the liver by retinoic acid acting via retinoic acid receptor-γ. J. Biol. Chem. 2010; 285:19002–19011. [PubMed: 20410309]
55. Geurts L, Muccioli GG, Delzenne NM, Cani PD. Chronic endocannabinoid system stimulation induces muscle macrophage and lipid accumulation in type 2 diabetic mice independently of metabolic endotoxaemia. PLoS ONE. 2013; 8:e55963. [PubMed: 23393605]
56. Grapov D, Adams SH, Pedersen TL, Garvey WT, Newman JW. Type 2 diabetes associated changes in the plasma non-esterified fatty acids, oxylipins and endocannabinoids. PLoS ONE. 2012; 7:e48852. [PubMed: 23144998]
57. Mehran AE, et al. Hyperinsulinemia drives diet-induced obesity independently of brain insulin production. Cell Metab. 2012; 16:723–737. [PubMed: 23217255]
58. Tang Y, et al. Beneficial metabolic effects of CB1R anti-sense oligonucleotide treatment in diet-induced obese AKR/J mice. PLoS ONE. 2012; 7:e42134. [PubMed: 22870290]
59. Maedler K, et al. Glucose-induced beta cell production of IL-1β contributes to glucotoxicity in human pancreatic islets. J. Clin. Invest. 2002; 110:851–860. [PubMed: 12235117]
60. Louvet A, et al. Cannabinoid CB2 receptors protect againsl alcoholic liver disease by regulating Kupffer cell polarization in mice. Hepatology. 2011; 54:1217–1226. [PubMed: 21735467]
61. Wang L, Liu J, Harvey-White J, Zimmer A, Kunos G. Endocannabinoid signaling via cannabinoid receptor 1 is involved in ethanol preference and its age-dependent decline in mice. Proc. Natl. Acad. Sci. USA. 2003; 100:1393–1398. [PubMed: 12538878]
62. Chorvat RJ, Berbaum J, Seriacki K, McElroy JF. JD-5006 and JD-5037: peripherally restricted (PR) cannabinoid-1 receptor blockers related to SLV-319 (Ibipinabant) as metabolic disorder therapeutics devoid of CNS liabilities. Bioorg. Med. Chem. Lett. 2012; 22:6173–6180. [PubMed: 22959249]
63. Folch J, Lees M, Sloane Stanley GH. A simple method for the isolation and purification of total lipides from animal tissues. J. Biol. Chem. 1957; 226:497–509. [PubMed: 13428781]
64. Godlewski G, et al. Inhibitor of fatty acid amide hydrolase normalizes cardiovascular function in hypertension without adverse metabolic effects. Chem. Biol. 2010; 17:1256–1266. [PubMed: 21095576]
65. Mukhopadhyay B, et al. Hyperactivation of anandamide synthesis and regulation of cell-cycle progression via cannabinoid type 1 (CB1) receptors in the regenerating liver. Proc. Natl. Acad. Sci. USA. 2011; 108:6323–6328. [PubMed: 21383171]
66. Buettner C, et al. Severe impairment in liver insulin signaling fails to alter hepatic insulin action in conscious mice. J. Clin. Invest. 2005; 115:1306–1313. [PubMed: 15864350]
67. Ju C, Pohl LR. Immunohisrochemical detection of protein adducts of 2, 4-dinitrochlorobenzene in antigen presenting cells and lymphocytes after oral administration to mice: lack of a role of Kupffer cells in oral tolerance. Chem. Res. Toxicol. 2001; 14:1209–1217. [PubMed: 11559035]
68. Tesz GJ, et al. Glucan particles for selective delivery of siRNA to phagocytic cells in mice. Biochem. J. 2011; 436:351–362. [PubMed: 21418037]
69. Rosenr ED, et al. Targeted elimination of peroxisome proliferator-activated receptor γ in β cells leads to abnormalities in islet mass without compromising glucose homeostasis. Mol. Cell Biol. 2003; 23:7222–7229. [PubMed: 14517292]
70. Liu J, et al. Lipopolysaccharide induces anandamide synthesis in macrophages via CD14/MAPK/phosphoinositide 3-kinase/NF-κB independently of platelet-activating factor. J. Biol. Chem. 2003; 278:4E034–46039.
71. Varga K, Wagner JA, Bridgen DT, Kunos G. Platelet- and macrophage-derived endogenous cannabinoids are involved in endotoxin-induced hypotension. FASEB J. 1998; 12:1035–1044. [PubMed: 9707176]

NIH-PA Author Manuscript
NIH-PA Author Manuscript
NIH-PA Author Manuscript

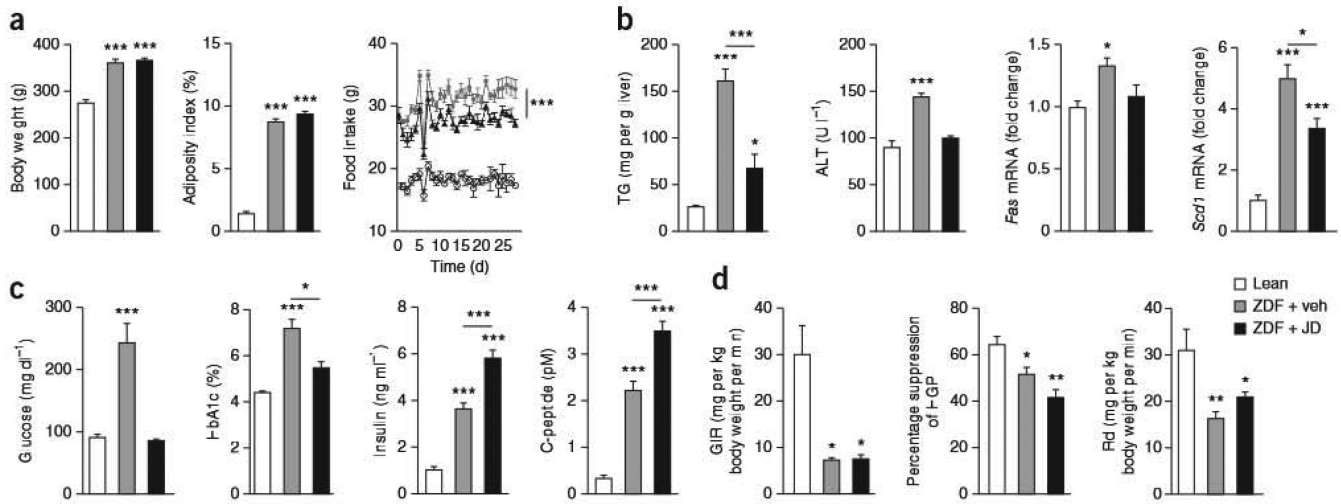

Figure 1.

Effects of peripheral CB_1R blockade on body weight, adiposity, hepatic lipogenesis and glycemic control in ZDF rats. Eight-week-old male ZDF rats treated for 28 d by oral gavage with 3 mg per kg body weight per day JD5037 or vehicle, (**a**) Effects of vehicle (gray columns and squares) and JD5037 (black columns and triangles) treatment of ZDF rats on body weight, adiposity and food intake compared to lean controls (white columns and open circles), *n*-20 pergroup. (**b–d**) Effects of vehicle (gray) and JD5037 (black) treatment of the same ZDF rats compared to lean controls (white) on hepatic triglycerides (FG), plasma alanine aminotransferase (ALT) and hepatic *Fas* and *Scd1* (**b**; $n = 20$ per group); on fasting blood glucose, HbA1c plasma insulin and C-peptide levels (**c**; $n = 20$ per group), and on the glucose-infusion rate (GIR), the percentage of suppression of hepatic glucose production (HGP) and the rate of glucose disappearance (Rd) during a euglycemic-hyperinsuiinemic clamp (**d**; $n = 5$ per group). Data are expressed as means means ± s.e.m. from 20 rats pergroup; * $P < 0.05$, ** $P < 0.01$, *** $p < 0.001$.

NIH-PA Author Manuscript
NIH-PA Author Manuscript
NIH-PA Author Manuscript

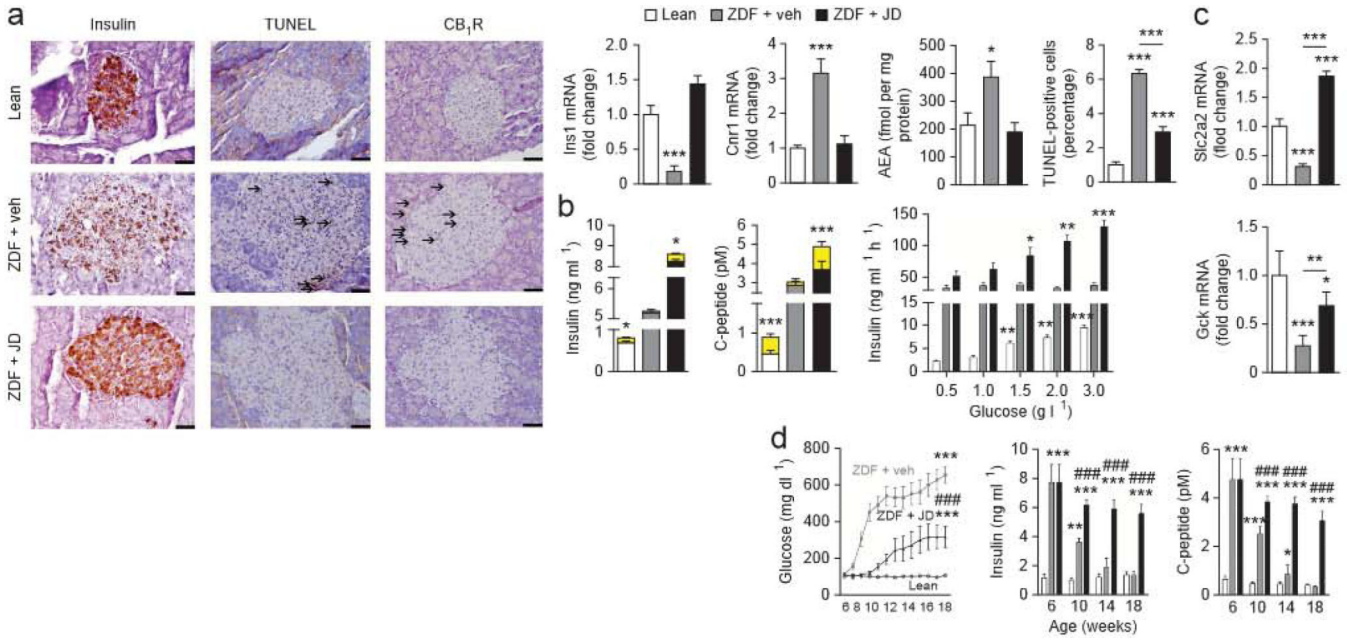

Figure 2.

The effect of chronic JD5037 treatment on beta cell survival and function in ZDF rats, (**a–d**) Treatments, as described in **Figure 1**, were started in 8-week-old diabetic rats (**a–c**) or 6-week-old prediabetic ZDF rats (**d**), (**a**) Immunohistochemical identification of insulin, TUNEL-positive cells and CB_1R protein in islets from lean rats and ZDF rats treated with vehicle or JD5037 for 4 weeks. Bar graphs show *Ins1* and *Cnr1* mRNA levels and anandamide (AEA) content of isolated islets or the percentage of TUNEL-positive cells; n = 15 rats per group. Arrows mark antigen-positive cells; significant difference from lean control, * $P < 0.05$, *** $P < 0.001$, (**b**) Glucose-induced insulin and C-peptide release *in vivo* (left and middle) or in isolated islets (right) from lean, vehicle-treated ZDF or JD5037-treated ZDF rats. In the left and middle graphs, the yellow segment indicates the glucose-induced increase in plasma insulin or C-peptide, respectively, over baseline insulin levels shown in white, gray or black; n = 10 rats or 8 islet preparations per group; * $P < 0.05$, ** $P < 0.01$, *** $P < 0.001$ relative to basel ine plasma insulin level or value in corresponding group of islets on 0,5 gl^{-1} glucose, (**c**) *Slc2a2* and *Gck* expression in islets from lean, vehicle-treated or JD5037-treated ZDF rats; n = 10 preparations per group; Pvalues as in a. (**d**) Baseline blood glucose, insulin and C-peptide levels in 6-week-old prediabetic ZDF rats and their biweekly change during 12 weeks of daily treatment with vehicle (gray columns and squares) or JD5037 (black columns and triangles). Mean ± s.e.m. values in age-matched lean controls are shown by white columns and open circles; n = 10 rats per group during weeks 6–18. Significant difference from corresponding value in lean (* $P < 0.05$, ** $P < 0.005$ or *** $p < 0.001$) or vehicle-treated (### $P < 0.001$) ZDF rats. Scale bars, 50 μm.

NIH-PA Author Manuscript
NIH-PA Author Manuscript
NIH-PA Author Manuscript

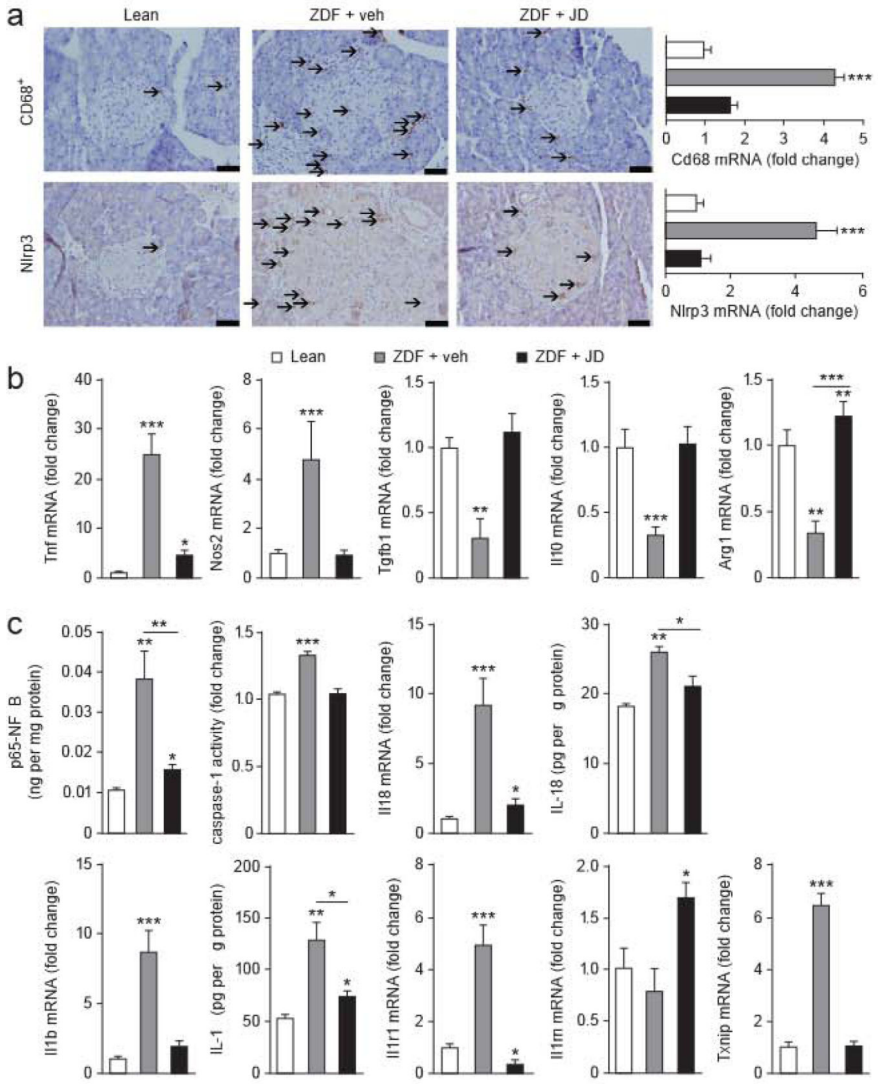

Figure 3.

Macrophage content and Mrp3 expression in islets of lean and diabetic rats, (**a**) Immunohistochemical stains for $CD68^{+}$ and Nlrp3 in islets of lean, ZDF and JD5037-treated ZDF rats; arrows mark antigen-positive cells. Scale bars, 50 μm. CD68 and *Nlrp3* mRNA levels measured in isolated islets are shown on the right, (**b**) Pro- and anti-inflammatory gene expression in the same islets as in **a**. (**c**) Expression of *Il18*, *Il1b*, *Il1r*, *Il1rn* and *Txnip*, as well as p65-NFκB, IL-18 and IL-1β protein and caspase-1 activity, in the same isets. Eight-week-old ZDF rats treated for 28 d with vehicle or JD5037 13 mg per kg body weight per day), with age-matched lean controls; $n = 20$ rats per group; * $P < 0.05$, ** $P < 0.01$, *** $P < 0.001$. Scale bars, 50 μm. Data are expressed as means + s.e.m.

NIH-PA Author Manuscript
NIH-PA Author Manuscript
NIH-PA Author Manuscript

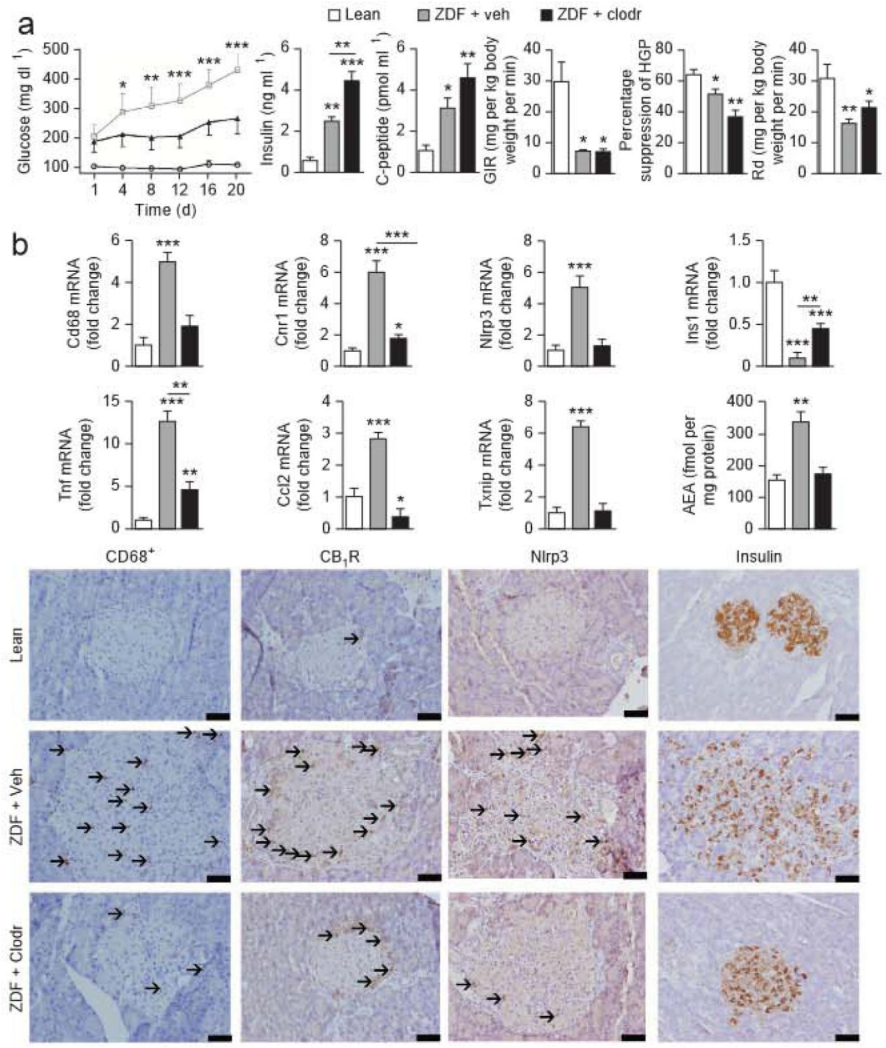

Figure 4.

Effects of macrophage depletion on glycemic control and proinflammatory signaling in islets of ZDF rats, (**a**) Blood glucose, insulin and C-peptide levels and insulin resistance analyzed by insulin clamps in lean littermate controls (white columns or circles) and In ZDF rats treated with empty liposomes (rah, gray col umns or squares) or clodronate-containing liposomes (clodr, black columns or triangles) Glycemic control was monitored for 20 d. (**b**) Top, mRNA expression of *Cd68* (as a marker of macrophages), *Cnr1*, *Nlrp3*, *Ins1*, *Tnf*, *Ccl2*, *Txnip* and anandamide content of islets isolated from pancreata of lean littermate rats (white columns) and ZDF rats treated with empty liposomes (veh, gray columns) or clodronate (clodr, black columns). Co umns and bars represent means ± s.e.m. from eight rats per group; ** $P < 0.01$, *** $p < 0.001$ relative to lean group, Bottom, representative immunohistochemistry stains (top) for CD68, CB_1R, Nlrp3 and insulin protein expression in pancreatic sections from lean control rats and ZDF rats treated with empty liposomes or clodronate. Arrows mark antigen-positive cells. Scale bars, 50 mμ.

NIH-PA Author Manuscript
NIH-PA Author Manuscript
NIH-PA Author Manuscript

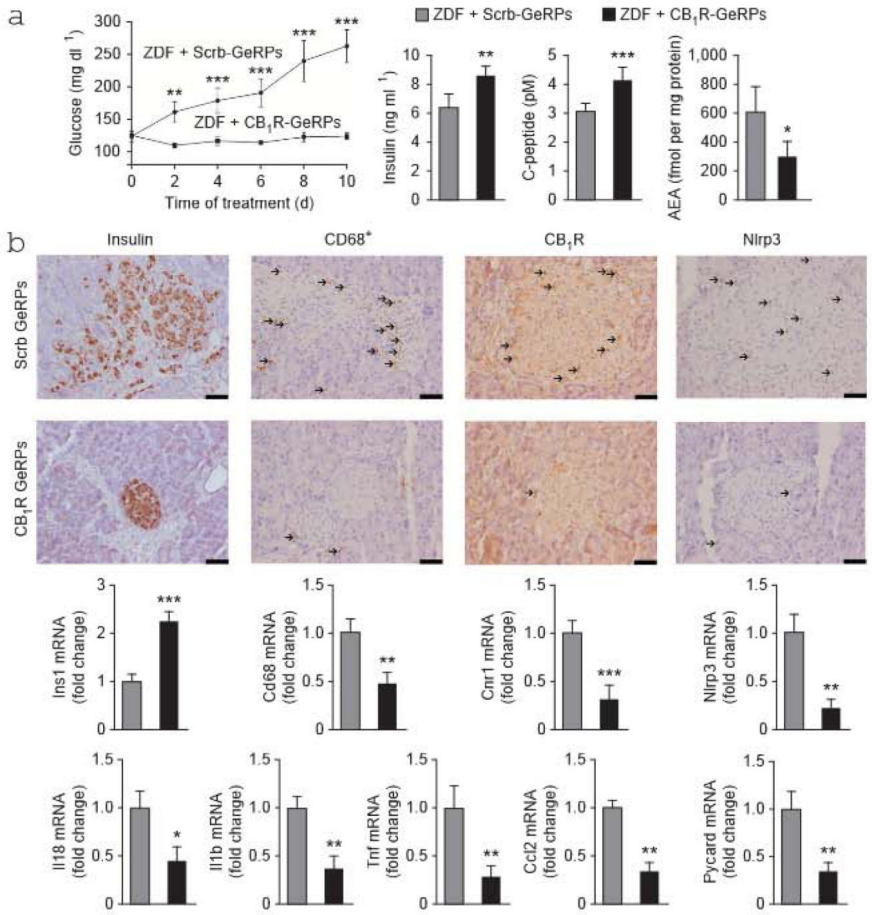

Figure 5.

Effects of macrophage-selective siRNA knockdown of CB_1R in ZDF rats, (**a**) Baseline blood glucose in 8-week-old ZDF rats during 10 d of treatment with scrambled (Scrb) GeRPs (gray columns and circles) or CB_1R GeRPs (black columns and squares) and plasma insulin, C-peptide and pancreatic AEA levels at end of treatment, n = 6–8 rats per group; * $P < 0.05$, ** $P < 0.01$, *** $P < 0.001$. (**b**)Top, immunohistochemistry stains for islet insulin, macrophages and CB_1R and Nlrp3 protein (with arrows marking antigen-positive cells). Scale bars, 50 μm. Bottom, mRNA expression of *Ins1*, *Cd68*. *Cnr1*, *Nlrp3*, *Il18*, *Il1b*, *Tnf*, *Ccl2* and *Pycard* in islets isolated from ZDF rats treated with scrambled (gray) or CB_1R GeRPs (black); n = 6 pergroup. * $P < 0.05$, ** $P < 0.01$, *** $p < .001$. Data are expressed as means ± s.e.m.

NIH-PA Author Manuscript

NIH-PA Author Manuscript

NIH-PA Author Manuscript

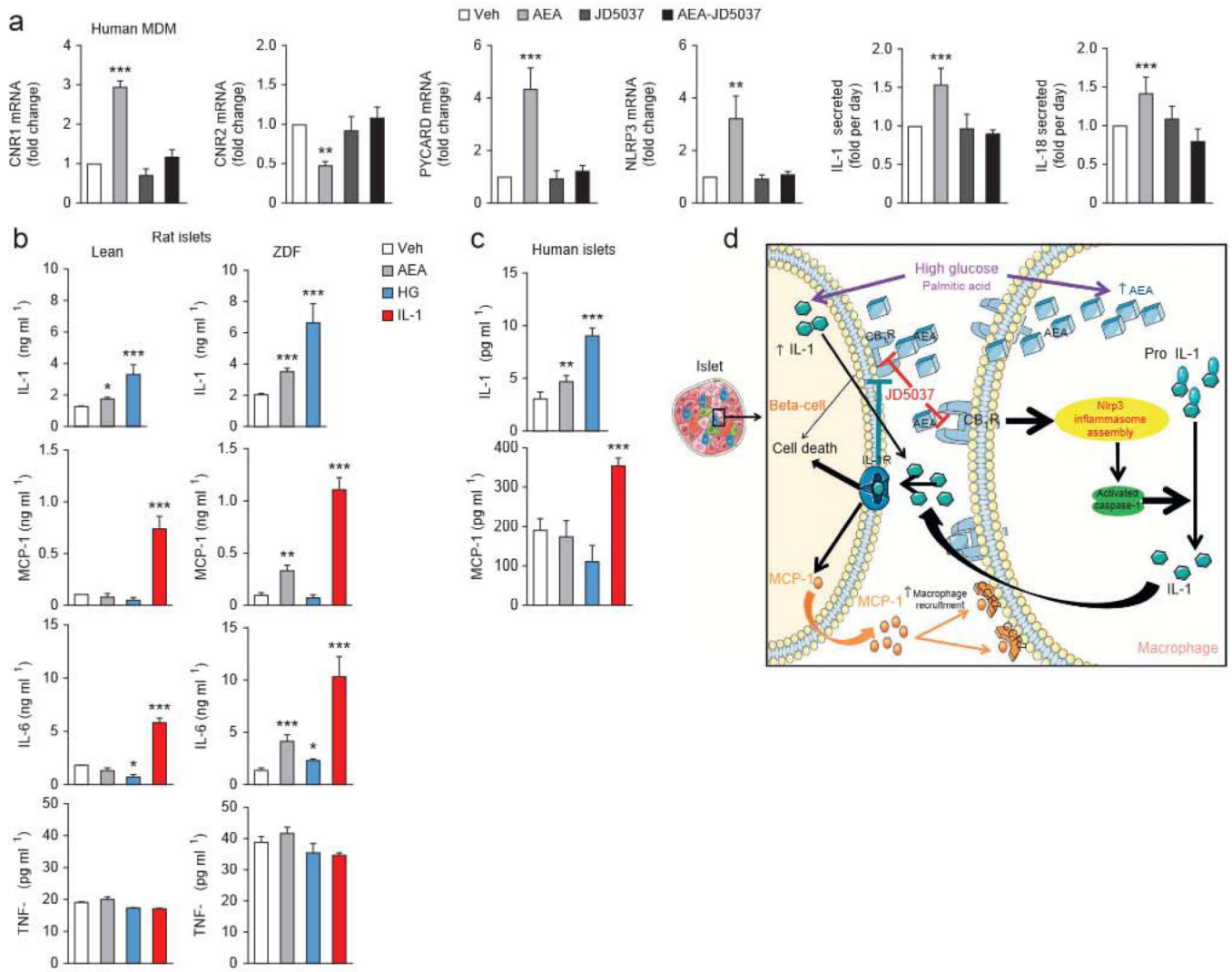

Figure 6.

Proinflammatory gene and protein expression in human macrophages and rat and human isolated islets treated with AEA, IL-1β or high giucose. (**a**) Relative effects of AEA (1 μM; light gray), JD5037 (100 nM; dafk gray) or their combination (biack) versus a vehicle control (veh; white) on *CNR1*, *CNR2*, *PYXARD* and *NLRP3* and on IL-1β and IL-18 secretion in human peripheral macrophages. Data are expressed as means ± s.e.m. from cells from six to eight different donors. MDM, monocyte-derived macrophages, (**b**) Effects of AEA (1 μM; light gray), high glucose HG; blue (33 mM) and IL-1β (30 ng ml^{-1}; red) versus a vehicle control (veh; white) on the secretion of IL-1β, MCP-l, IL-6 and TNF-α by islets from lean and ZDF rats, (**c**) Effects of vehicle, AEA, high glucose and IL-1β on IL-1β and MCP-l secretion by human islets. Data in b and c are expressed as means ± s.e.m. from six to eight preparations, each containing ten islets. (**d**) Schematic illustration of the mechanism of CB_1R-mediated beta cell loss in the diabetic islet, This figure was prepared using a template on the Servier medical art website {http://www.servier.frirservier-medical-art).